# Subthalamic Nucleus Activation Occurs Early during Stopping and Is Associated with Trait Impulsivity

**Jong H. Yoon[1,2], Edward Dong Bo Cui[3], Michael J. Minzenberg[4], and Cameron S. Carter[5]**

## Abstract

■ The subthalamic nucleus (STN) is thought to be a central regulator of behavioral inhibition, which is thought to be a major determinant of impulsivity. Thus, it would be reasonable to hypothesize that STN function is related to impulsivity. However, it has been difficult to test this hypothesis because of the challenges in noninvasively and accurately measuring this structure's signal in humans. We utilized a novel approach for STN signal localization that entails identifying this structure directly on fMRI images for each individual participant in native space. Using this approach, we measured STN responses during the stop signal task in a sample of healthy adult participants. We confirmed that the STN exhibited selective activation during "Stop" trials. Furthermore, the magnitude of STN activation during successful Stop trials inversely correlated with individual differences in trait impulsivity as measured by a personality inventory. Time course analysis revealed that early STN activation differentiated successful from unsuccessful Stop trials, and individual differences in the magnitude of STN activation inversely correlated with stop signal RT, an estimate of time required to stop. These results are consistent with the STN playing a central role in inhibition and related behavioral proclivities, with implications for both normal range function and clinical syndromes of inhibitory dyscontrol. Moreover, the methods utilized in this study for measuring STN fMRI signal in humans may be gainfully applied in future studies to further our understanding of the role of the STN in regulating behavior and neuropsychiatric conditions. ■



## INTRODUCTION

A fundamental aspect of behavioral control is the ability to inhibit action. A related construct is impulsivity, which can be defined as the tendency to make rash or reflexive actions that are potentially maladaptive, such as running out onto a busy street in pursuit of ball or blurting out inappropriate or offensive statements. Some models of impulsivity invoke the failure of behavioral inhibition as one of the core mechanisms underlying impulsive action (de Wit, 2009). Impulsivity is associated with a broad array of maladaptive behaviors or conditions with high public health impact such as attention-deficit/hyperactivity disorder (Barkley, 1997), bipolar disorder (Strakowski et al., 2010; Swann, Lijffijt, Lane, Steinberg, & Moeller, 2009), substance abuse (Ersche, Turton, Pradhan, Bullmore, & Robbins, 2010), and suicide (Horesh, Gothelf, Ofek, Weizman, & Apter, 1999; Nock & Kessler, 2006). Thus, the elucidation of the brain mechanisms underlying behavioral inhibition would advance our understanding of a fundamental determinant of behavior and important neuropsychiatric conditions and states.

Although a network of brain regions regulates inhibition, convergent lines of research suggest that the subthalamic nucleus (STN) is a particularly important structure within this network in humans (Obeso et al., 2014; Forstmann et al., 2012; Bickel et al., 2010; Eagle et al., 2008; Li, Yan, Sinha, & Lee, 2008; Frank, Samanta, Moustafa, & Sherman, 2007; Aron & Poldrack, 2006). However, basic questions about the role of the STN in behavioral inhibition in humans remain unresolved. Although prior fMRI studies have documented ventral midbrain activations consistent with STN engagement during conditions requiring inhibition of action (Li et al., 2008; Aron & Poldrack, 2006), the mechanisms by which STN signaling mediates inhibition remain unresolved. Moreover, STN's influence and impact on human behavior is unclear. Although the STN has been linked with various laboratory-based measures of behaviors and behavioral tendencies involving inhibitory control in humans (Forstmann et al., 2012; Li et al., 2008; Aron & Poldrack, 2006), particularly in the context of Parkinson disease (Obeso et al., 2014; Bickel et al., 2010; Frank et al., 2007), it is unclear whether and how profoundly STN function impacts real-world behaviors or behavioral proclivity in nonpatient populations.

A major challenge facing efforts to better understand STN function in humans is the difficulty in measuring this structure's signal noninvasively. The STN's small size and location abutting other nuclei within the ventral midbrain

[1]Stanford University, [2]Veterans Affairs Palo Alto Health Care System, [3]Case Western Reserve University, [4]University of California, Los Angeles, [5]University of California, Davis

means not only that the STN's signal is very low but also that measurements of its signal are susceptible to contamination from nearby structures, such as the substantia nigra (SN; de Hollander, Keuken, & Forstmann, 2015). These factors reduce measurement accuracy, raise questions of the misattribution of function to the STN, and limit our ability to deduce the functional properties of the STN. Thus, improved methods for accurately measuring STN activity could lead to new insights into its function. The importance of accurately measuring STN signal is also highlighted by the increasing relevance of this structure in therapeutics. The STN is now a major treatment target for deep brain stimulation in Parkinson disease (Bronstein et al., 2011) and STN deep brain stimulation is U.S. Food and Drug Administration-approved for treatment refractory obsessive-compulsive disorder. Improvements in measuring the functional properties of the STN could help to refine these treatments.

We recently developed a novel approach for measuring STN BOLD signal at the individual participant level (Yoon et al., 2015). This approach involves identifying the STN for each individual directly on EPI volumes, which may improve the accuracy of STN signal detection. We undertook this study to validate this method and gain novel insights into STN's role in inhibition and human behavior. We sought to validate this method by testing whether our method detects the selective engagement of the STN during events thought to potently drive STN activity, such as Stop trials of the stop signal task (SST; Li et al., 2008; Aron & Poldrack, 2006; Logan, Cowan, & Davis, 1984). This task also provided an opportunity to test whether differential STN activation occurs in successful compared with unsuccessful stop trials. Differential activation would support the proposition that the STN directly contributes to stopping. Finally, we tested whether STN shapes a broad array of human behaviors associated with inhibition by determining whether individual differences in STN activation predict trait impulsivity as measured by a well-validated personality inventory.

## METHODS

### Participants

Eighteen right-handed adult participants (mean age = 30.7 ± 3.9 years, 50% men) completed this study. Exclusion criteria for all participants were history of major psychiatric illness (determined by the Structured Clinical Interview for *Diagnostic and Statistical Manual of Mental Disorders, 4th Ed., Text Revision* Disorders, Nonpatient version, administered by trained diagnosticians) or neurological illness, IQ of less than 70 (determined by the Wechsler Abbreviated Scale of Intelligence), drug and/or alcohol dependence history or abuse in the previous 3 months, a positive urine drug screen on the day of testing, clinically significant head trauma, current use of any psychotropic medication, or any known contraindication to MRI. After complete description of the study, informed consent was obtained, and participants were compensated for their participation. This study was approved by the institutional review board at the University of California, Davis.

### Cognitive Paradigm

Participants performed the SST during fMRI (Figure 1), which measures the participant's ability to inhibit motor responses. There are two conditions in this task: "Go" and "Stop." Trials for both conditions begin with the appearance of a white circular ring in the center of a black background screen. After 500 msec, an arrowhead pointing right or left, randomized with 50% probability, is shown within this ring. This indicates to the participant that he or she is to respond with a right or left button press using his or her middle or index finger, corresponding to either the left or rightward pointing arrow, respectively. The participants are instructed to make a response within 1 sec of the appearance of the arrow. The ring and arrowhead remain on the screen for 1 sec, unless a response is registered within this time period,

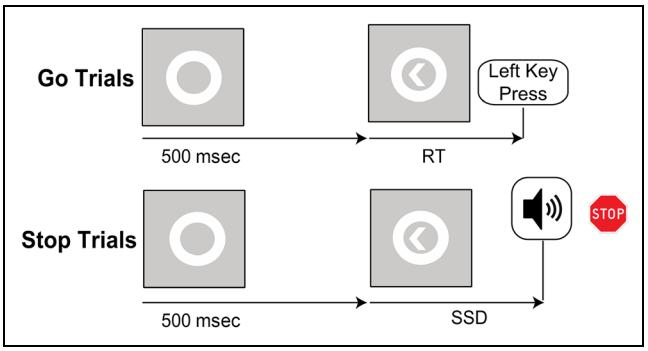


**Figure 1.** Stop signal task (SST) description. (A) There are two conditions in this task: Go and Stop. Trials for both conditions begin with the appearance of a white circular ring in the center of a black background screen. After 500 msec, an arrowhead pointing right or left, randomized with 50% probability, is shown within this ring. This indicates to the participant that he or she is to respond with a right or left button press using his or her middle or index finger, corresponding to either the left or rightward pointing arrow, respectively. The participants are instructed to make a response within 1 sec of the appearance of the arrow. The ring and arrowhead remain on the screen for 1 sec unless a response is registered within this time period, in which case the stimuli disappear. The intertrial interval consists of a black screen and its duration is jittered between 0.5 and 4 sec, with a mean of 1 sec and a frequency drawn from an exponential distribution. The Stop trials are identical to the Go trials except for the presentation of an auditory stimulus (900 Hz, duration = 500 msec), which is presented after a short delay following the presentation of the arrow stimulus and signals the need to withhold the response. This SSD varies dynamically throughout the experiment, based on the participant's performance. A successful or unsuccessful inhibition results in the shortening or lengthening or of the SSD in subsequent trials. A staircasing algorithm ensures convergence to a probability of inhibition of 50% by the end of the experiment. Thus, there were two types of Stop trials, Stop Inhibit and Stop Respond.

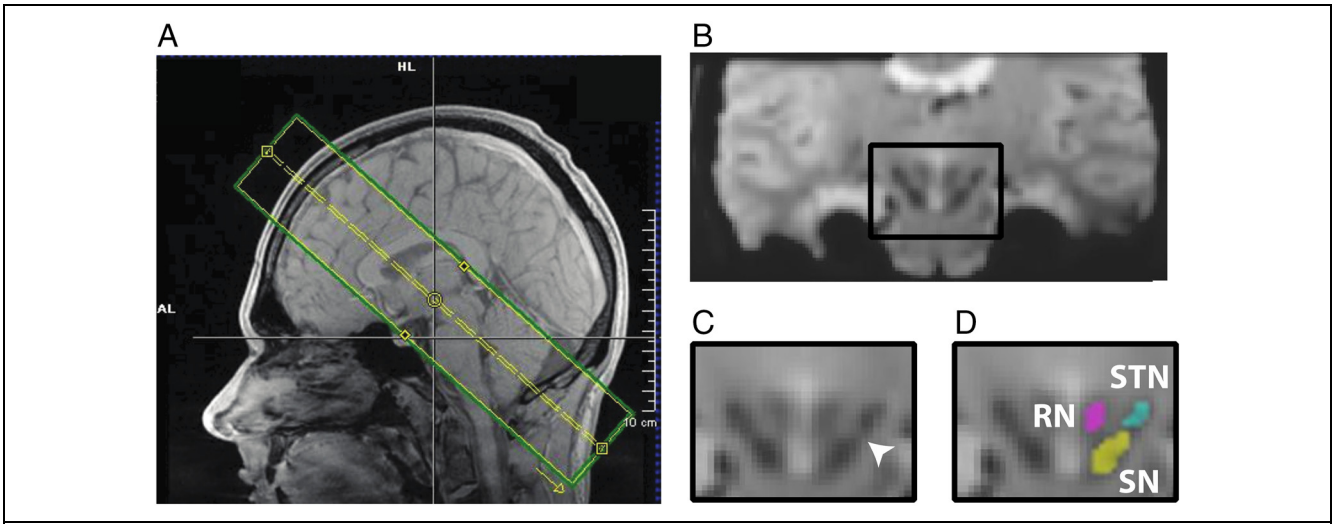


**Figure 2.** Localizing fMRI signal from the STN. (A) A sagittal view of a T1 structural image of a participant with an outline in green showing the in-plane extent of EPI acquisition volume. (B) Coronal section from a task EPI volume, which illustrates that the STN can be distinguished from its neighbors in the ventral midbrain. The black box outlines the midbrain region shown in C and D. Close-up of the midbrain region showing areas of hypointensity due to the dephasing effects of high iron in the red nucleus (RN; magenta), substantia nigra (SN; yellow), and STN (blue). The white arrow points to the gap separating the SN and the STN that can only be visualized in a coronal section that is orthogonal to the AC–PC plane.

in which case the stimuli disappear. Stop trials are identical to the Go trials, except for the presentation of an auditory stimulus (900 Hz, duration = 500 msec), which signals the need to withhold the response. The auditory stimulus is presented shortly after the appearance of the arrow, and the delay interval between these stimuli is referred to as the stop signal delay (SSD). The SSD varies dynamically throughout the experiment based on the participant's performance. Successful or unsuccessful inhibition in a trial results in the shortening or lengthening, with 50-msec steps, of the SSD in subsequent trials, respectively. A staircasing algorithm ensures convergence to a probability of inhibition of 50% by the end of the experiment. Thus, approximately half of Stop trials were ones in which participants successfully stopped their responses ("Stop Inhibit"), and the other half were ones in which they did not inhibit their responses ("Stop Respond"). All responses were executed with the right hand. There were 64 Stop trials and 192 Go trials.

### Measurement of Impulsivity

We quantified each participant's level of impulsivity from the Temperament and Character Inventory (TCI), computerized version (Cloninger, 1994). Participants completed this self-report inventory designed to measure facets and dimensions of personality. In the TCI, impulsivity is a facet or subscale within the Novelty Seeking temperament domain.

### fMRI Acquisition and Processing

All data were collected at the University of California, Davis, Imaging Research Center. The visual stimuli were displayed on a projection screen and viewed by participants through a mirror attached to the head coil. Foam padding stabilized the participant's head in the head coil to minimize head motion during the experiment. Functional scans (T2* weighted, gradient recalled echo–EPI, repetition time [TR] = 2000 msec, echo time = 34 msec, flip angle = 75°, field of view = 224 mm × 224 mm with 25 contiguous slices (zero gap) in the axial oblique plane, voxel size of 1.8 × 1.8 × 1.9 mm) were acquired on a 3-T Siemens TIM Trio MRI System with a 32-channel phased-array head coil (Siemens HealthCare). To provide full coverage of the midbrain and maximize coverage of relevant cortical regions, the volume of acquisition was established with axial-oblique slices arranged at an angle that was approximately 45° from the AC–PC plane. The image volume was centered over the midbrain to ensure full coverage of this region (Figure 2A). Preprocessing, implemented in SPM8, included temporal and spatial realignment to correct for slice acquisition timing differences and head movement, respectively. We inspected the linear movement parameters that are produced from the spatial realignment procedure in SPM for the presence of greater than 2 mm within-run head movement in any direction. No participant displayed such movement, and thus, no participants were removed for excessive movement.

Note that, for ROI-based analyses described below, EPI images did not undergo spatial smoothing or spatial normalization for coregistration with a template brain. Instead, all analyses were conducted in the participant's "native space" to avoid problems in localization that could arise from these procedures. For voxel-wise general linear model (GLM)-based analyses, images underwent spatial smoothing as described below.

### Segmenting the STN ROI

We developed a novel approach for the localization of STN fMRI signal, which was first reported in a prior report (Yoon et al., 2015). The STN has a high concentration of iron (Dormont et al., 2004) and appears as a discrete region of hypointensity in a characteristic location in the ventral midbrain on EPI images (Richter, Hoque, Halliday, Lozano, & Saint-Cyr, 2004; Figure 2). These features allowed us to identify each participant's STN on his or her unsmoothed EPI volumes in "native space" (Figure 2) and to construct binary masks of the STN using a semiautomated procedure. We derived task-evoked signal estimates of the STN with these masks. This procedure minimized signal localization errors that may result from spatial smoothing or coregistration of fMRI volumes to an individual's structural MRI or normalization onto a template space such as the MNI brain. It is important to note that our method distinguished the STN from the substantial nigra (SN; Yoon et al., 2015), thus minimizing the measured STN signal being contaminated by SN signal (de Hollander et al., 2015).

The first step in our procedure for creating a mask of the STN was to generate an optimal EPI volume for visualizing and creating an ROI mask of the STN. We first created an average EPI image from a 10-min resting-state scan that each participant completed during the same session in which the SST scan was acquired. The resting-state scan utilized the same EPI scanning parameters as the SST scan. We segmented the STN from the resting-state scan to avoid any bias that may occur if segmentations were derived from the SST scans. We then resliced the averaged EPI volume in an axial plane parallel to the AC–PC line using trilinear up-sampling. Next, we generated coronal sections orthogonal to the AC–PC-aligned axial plane, which brings into view a hyperintense region that separates the STN from the SN (Schafer et al., 2011; Coenen, Prescher, Schmidt, Picozzi, & Gielen, 2008). The SN also has a high concentration of iron and appears hypointense on EPI images (Haacke et al., 2005; Dexter et al., 1991; Sofic, Paulus, Jellinger, Riederer, & Youdim, 1991). We utilized ITK-Snap (Yushkevich et al., 2006) to view the coronal images and segment the STN. Image contrast for visualizing ROIs was optimized by setting the minimal (level) and maximal (window) voxel intensities to the 1st and 99th percentiles of voxel intensity distribution, modifying the control point for the function relating input versus output voxel intensities and filtering voxel intensities. We then generated the initial automated segmentations for the STN using the default settings for ITK-Snap's Snake toolbox.

These initial segmentations underwent manual inspection and editing. The reslicing of images in AC–PC-aligned planes brought them into register with the Schaltenbrand and Wahren Brain Atlas (Schaltenbrand, Hassler, & Wahren, 1977). Although some limitations of this atlas have been documented (Niemann & van Nieuwenhofen, 1999), it is widely considered to reliably depict the location of the STN and other BG structures and is utilized by neurosurgeons to guide the targeting of the STN during deep brain stimulation implantations (Nowinski, 1998). We cross-referenced our segmentations with anatomic information provided by the Schaltenbrand and Wahren atlas.

The anterior extent of the STN segmentations was limited to 3 mm anterior to the midcommissural point to avoid the inclusion of the globus pallidus, which also appears hypointense on EPI volumes. In instances in which the hyperintense region separating the STN and SN cannot be unambiguously identified, the horizontal plane defined by the inferior border of the red nucleus in the anterior-most coronal slice that includes the red nucleus served as the boundary defining the superior and inferior extents of the SN and STN, respectively; the posterior extent of the STN was limited to 7 mm posterior to the midcommissural point.

### STN Temporal SNR Measurements

To calculate the temporal SNR (tSNR), we calculated the ratio between the mean and the standard deviation of a voxel's BOLD time series. This was done for all voxels within the right and left STN ROIs, and the results are averaged to yield the final voxel-wise tSNR.

### STN ROI fMRI Analysis

We obtained estimates of STN task-evoked responses in two complementary ways. Both approaches involved averaging signal estimates across all voxels in the STN ROI masks. The first method entailed obtaining beta weights from a multiple regression model of the STN BOLD signal. In this model, the SPM canonical hemodynamic response function was convolved with a series of delta functions, distinctly for Go, Stop Inhibit, and Stop Respond trials. The beta weights reflected the magnitude of STN signal for each trial type. We included a separate set of covariates for nonresponse and Go error trials and the six movement parameters. We also included the first temporal derivative of covariates in the regression matrix to account for potential differences in BOLD signal temporal dynamics associated with RT differences or other nuisance factors across individuals. Delta functions were positioned at the onset of the arrow stimulus presentation. This analysis was conducted in SPM8 with custom MATLAB (MathWorks) scripts to extract beta estimates.

The following comparisons were utilized for hypothesis testing in the regression-based analysis. For validating the study's method for STN signal localization, we sought evidence of selective engagement of the STN in trials requiring behavioral inhibition. Selective STN engagement was tested by comparing all Stop trials (Stop Respond and Stop Inhibit) with Go trials. Both Stop trial types were grouped together in this comparison because the

stop signal stimulus was presented, and therefore, inhibitory mechanisms were presumably engaged in both trial types. The inclusion of both trial types substantially increased the number of trials from which STN activation could be estimated and, therefore, would enhance power to detect true effects of interest. We also compared each Stop trial type with Go trials separately. The contrast of Stop Inhibit with Go trials was of particular relevance given the unique signifier of behavioral inhibition that these trials represent. Hypothesis testing of an association with impulsivity proceeded in a similar manner: We first correlated individual differences in STN signal during all Stop trials with impulsivity and then conducted correlations between each Stop trial type with impulsivity separately to determine whether Stop Inhibit or Stop Respond trials were differentially associated with impulsivity. The former was of particular interest and predicted to be inversely correlated with impulsivity given that STN activation in Stop Inhibit trials

The second method for measuring STN responses was the finite impulse response (FIR) method, which produced deconvolved estimates of trial-averaged BOLD time courses. These results can validate the regression-based analyses described above by confirming that the extracted fMRI signal from the ROI conforms to the well-characterized evoked BOLD signal. These results can also reveal subtle differences in the temporal pattern of STN activations across trial types that cannot be detected by the regression-based analyses. The main comparison examined in the time course data was between the Stop Respond and Stop Inhibit trials. Because these trials are identical in terms of task demands and differ only in success of inhibition of motor responses, this comparison could reveal subtle differences in the temporal pattern of STN signaling corresponding to successful inhibition. These data were obtained with custom-made MATLAB scripts. The FIR time course results are reported in terms of scans as the unit of time. One scan is equivalent to one TR or 2 sec. The first scan of the time series represents the BOLD signal occurring in the 0–2 sec time interval, whereby the 0 sec time point represents the start of a trial.

We utilized paired $t$ tests to compare levels of activity of the STN across trial types. Other statistical tests that were utilized are clearly noted in the manuscript. Two-tailed levels of significance were used to all analyses. Alpha levels were adjusted for multiple comparisons when appropriate.

### Voxel-wise, Whole-brain fMRI Analysis

We conducted, in parallel to the STN ROI analysis, voxel-wise mixed-model GLM-based analyses of task-evoked activity within the acquired EPI volume. We utilized the same set of preprocessing steps on EPI volumes for this analysis as was applied for the STN ROI analysis, with the addition of spatial smoothing with a 5-mm FWHM Gaussian kernel. At the single-participant level, we conducted a multiple regression analysis using the same procedure described above in the STN ROI multiple regression analysis, with covariates for Go, Stop Inhibit, and Stop Respond trials. The group-level analysis involved spatially normalizing the results of the single-participant level analysis. This was accomplished using a whole-brain EPI volume intermediary in the spatial normalization process. The partial brain task EPI volumes were first coregistered with these whole-brain EPI volumes, which were spatially normalized to the MNI brain. The normalization parameters were then applied to task EPIs for group averaging. This procedure was required because, in normalization of the partial brain, task volumes directly to the template brain would have introduced substantial errors in normalization and coregistration. Whole-brain EPIs were obtained for each and every participant after the acquisition of task EPI scans, and their acquisition parameters were identical to the task EPI scans except for a TR of 6 sec, which was required to allow for whole-brain acquisitions. Six whole-brain EPI scans were obtained and averaged. We employed cluster-wise control of family-wise error for significance testing with a cluster defining threshold of $p = .001$ (Eklund, Nichols, & Knutsson, 2016) and $k = 5$. The location of cortical activations was confirmed using the Anatomical Automatic Labeling atlas as implemented in SPM.

## RESULTS

### Behavioral Results

Eighteen right-handed healthy adult participants (mean age = 30.7 ± 3.9 years, 50% men) completed this study. Participants' behavioral performance on the SST is displayed in Table 1. All responses were executed with the right hand.

### STN tSNR

The mean voxel-wise tSNR were 39.5 (±5.2) and 38.5 (±6.5) within the left and right STN ROIs, respectively.

**Table 1.** Behavioral Measures

| | |
|---|---|
| Mean correct Go RT (msec) | 416 (86) |
| Mean Stop Respond RT (msec) | 373 (62) |
| Go errors (%) | 3.3 (2.5) |
| Mean SSD (msec) | 218 (86) |
| Percent inhibition | 48.4 (5.5) |
| SSRT (msec) | 198 (44) |

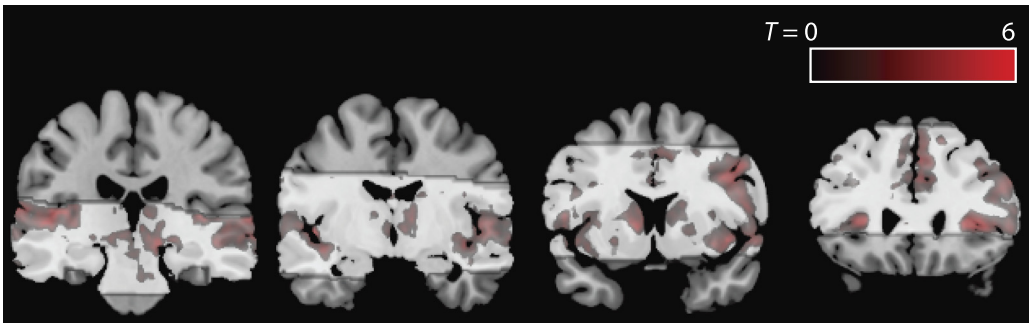


**Figure 3.** Voxel-wise GLM results. This figure shows areas of activation in the Stop Inhibit–Go contrast, threshold of $p = .001$. The extent of fMRI coverage is indicated by the lightly shaded regions. Details of coordinates and statistics for these regions can be found in Table 1.

### fMRI Results—Voxel-wise GLM

We observed significant activation during the Stop Inhibit compared with Go trials in the following brain regions: superior temporal gyrus, insula, inferior gyrus pars opercularis, medial prefrontal regions (SMA/ACC), striatum, dorsal midbrain, and thalamus (Figure 3 and Table 1). In the contrast between Stop Inhibit and Stop Respond trial types, no region exhibited signification activation (Table 2).

### fMRI Results—Selective Activation of the STN in Stop Trials

The left STN showed significantly elevated activation during Stop trials (Stop Inhibit and Stop Respond) compared with Go trials, $p = .022$ (Figure 4A). The difference between Stop Respond and Go trials was significant, $p = .010$, but the difference between Stop Inhibit and Go trials was not significant, $p = .252$. There was no significant difference between Stop Inhibit and Stop Respond trials

**Table 2.** Significant Activations (Stop Inhibit–Go)

| *p(FWE-cor)* | *k* | *Peak T* | *x y z (mm)* | *Region* |
|---|---|---|---|---|
| <.001 | 1986 | 11.63 | −46 −16 −2 | Superior temporal gyrus/insula |
| | | 10.93 | −32 22 4 | |
| | | 8.17 | −42 −28 8 | |
| <.001 | 4449 | 10.81 | 34 24 2 | Superior temporal gyrus/insula/inferior frontal gyrus |
| | | 10.28 | 42 4 36 | |
| | | 10.23 | 64 −22 8 | |
| <.001 | 946 | 8.88 | 8 22 42 | Medial frontal–SMA/ACC |
| | | 7.49 | 6 12 42 | |
| | | 7.43 | 6 24 30 | |
| <.001 | 442 | 7.77 | 12 −24 −6 | Dorsal brainstem/thalamus |
| | | 6.15 | 10 −12 4 | |
| | | 4.99 | 6 −16 14 | |
| .002 | 125 | 5.58 | −10 8 2 | Head of caudate |
| | | 4.55 | −16 8 8 | |
| .004 | 113 | 5.25 | −12 −24 −4 | Dorsal midbrain/thalamus |
| | | 5.15 | −4 −8 0 | |
| | | 5.01 | −4 −30 −14 | |
| .012 | 92 | 5.23 | −26 −72 −52 | Cerebellum |
| | | 4.15 | −18 −78 −52 | |

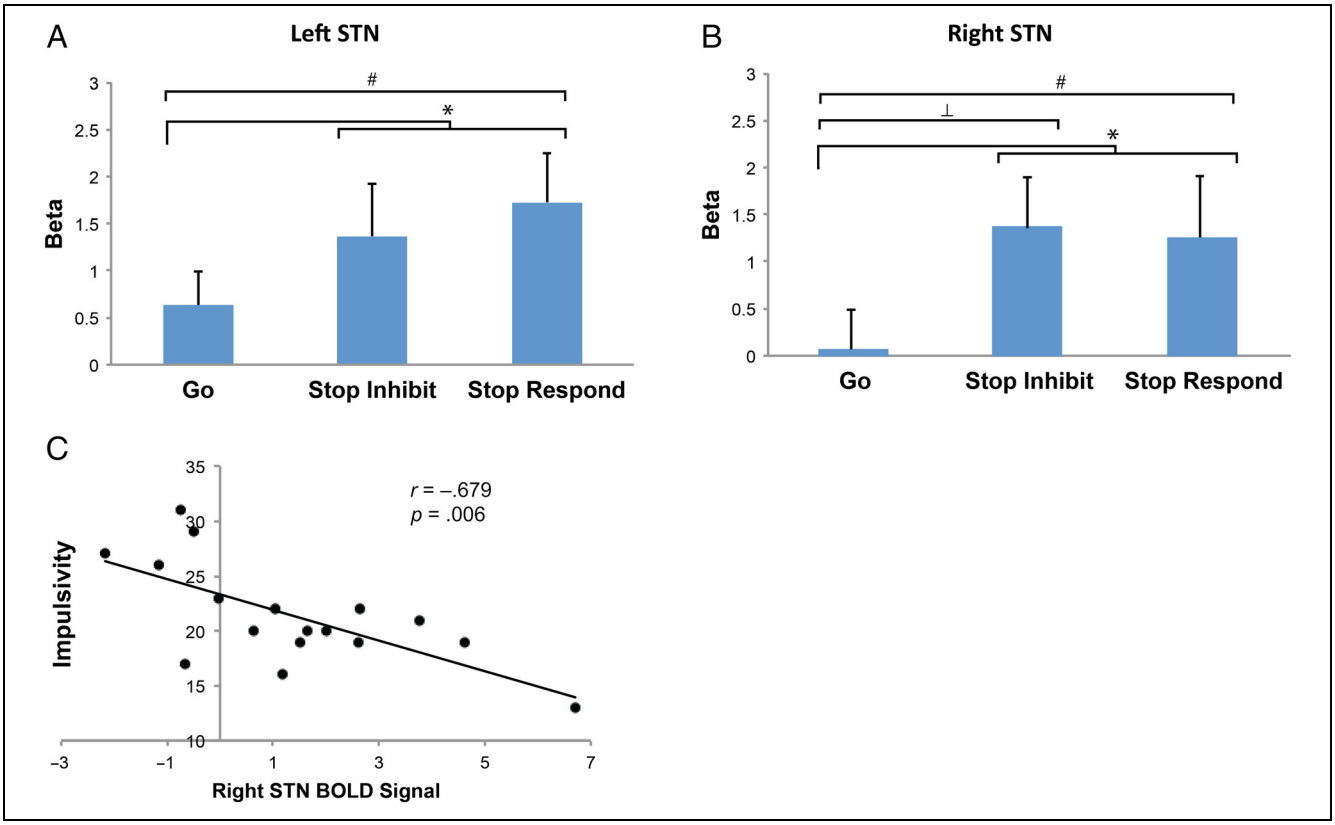


**Figure 4.** STN BOLD signal during the SST and association with impulsivity. (A) Results of the regression-based estimates of the left STN signal show higher activation in Stop trials compared with Go trials, $^{\#}p < .001$. STN signal in Stop Inhibit trials was significantly elevated compared with Go trials, $^{\perp}p = .024$, whereas Stop Respond trials showed nearly significant difference compared with Go trials, $^{\#}p = .052$. (B) Results of the regression-based estimates of the right STN signal show higher activation in Stop trials compared with Go trials, $^{\#}p < .011$. Stop Respond signal was higher than in Go trials, $^{\#}p = .010$. (C) There was a significant inverse correlation between right STN Stop Inhibit signal and TCI measure of impulsivity, $r = -.679$, $p = .006$.

in the left STN, $p = .469$. The right STN showed significantly elevated signal during Stop trials compared with Go trials, $p < .001$ (Figure 4B). When Stop Inhibit and Stop Respond trials were compared with Go trials separately, Stop Inhibit trials showed higher activation, $p = .024$, whereas Stop Respond trials did not, $p = .052$. The difference between Stop Inhibit and Stop Respond trials in the right STN was nonsignificant, $p = .881$. All $p$ values were adjusted for multiple comparisons.

### STN Correlation with Impulsivity

We tested if the level of STN signal was associated with individual differences in impulsivity score from the TCI (Cloninger, 1994). The signal from the right STN, but not the left STN, during Stop trials was significantly and inversely correlated with impulsivity, $r = -.580$, $p = .030$, and $r = -.348$, $p = .314$, corrected for multiple comparisons. The right STN correlation with impulsivity appeared to be driven by its activation during Stop Inhibit trials since this correlation was $r = -.679$, $p = .006$, whereas it was $r = -0.226$, $p = .734$, with Stop Respond trials. We also found evidence of personality dimension specificity, in that right STN BOLD signal did not correlate with two other dimensions within the Novelty Seeking domain, Extravagance and Disorderliness. The correlation with impulsivity was also region specific in that the signal from the right SN, another BG nucleus situated just ventral to the STN, whose signal was localized in the same manner as the STN (Yoon et al., 2015), was not significant. Furthermore, the correlation between right STN and impulsivity remained highly significant, $r = -.707$, $p = .006$, after controlling for right SN signal.

### STN Signal Time Course—Early Activation during Stop Inhibit Trials

We obtained trial-averaged deconcolved BOLD FIR time courses from the STN as a means of evaluating quality of fMRI data derived from our method for STN signal localization. Data quality is a concern given the relatively small signal that may be measurable from such small structures within the ventral midbrain. The overall BOLD time courses for both trial types were consistent with the well-characterized task-evoked BOLD signal for discrete

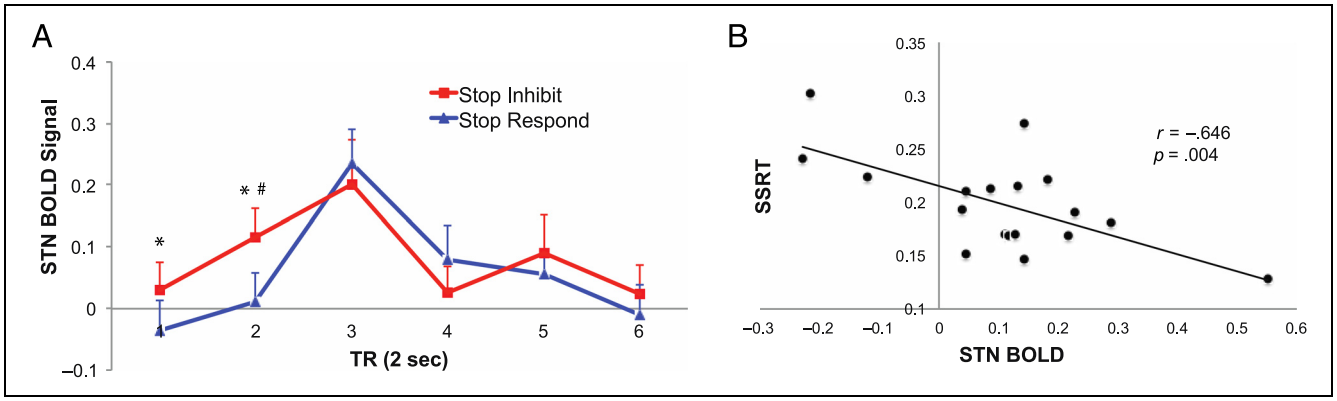


**Figure 5.** FIR time courses of STN BOLD signal during SST. Results from the left STN are displayed. The left STN showed early (Scans 1 and 2) enhanced activation in Stop Inhibit compared with Stop Respond trials, confirmed with a repeated-measures ANOVA showing significant effect of trial type, $^{*}p = .037$. This difference was driven by Scan 2 signal, $^{\#}p = .048$. (B) The differential left STN Scan 2 activation in Stop Inhibit compared with Stop Respond trials showed a significant inverse relationship with the SSRT. This association was not due to outliers (see text for details).

events (Glover, 1999). In both trial types, the BOLD signal progressively increased from baseline until their peaks at Scan 3 (approximately 4–6 sec after stimulus onset) and then returned to baseline. The relative magnitude of peaks was consistent with the regression-based results, Stop Inhibit = Stop Respond.

These time courses also provide an opportunity to explore the possibility of the presence of subtle differences in STN responses across trial types, which may be obscured in the regression-based estimates of STN responses. Indeed, the time course of left STN responses appeared to differ between Stop Inhibit compared with Stop Respond trials (Figure 5). The former showed higher signal early in the trial (Scans 1 and 2). This was confirmed with a repeated-measures ANOVA of Stop Inhibit and Stop Respond Scans 1 and 2, which showed a significant effect of trial type ($df(1, 17)$, $F = 5.094$, $p = .037$). This difference was driven mostly by Scan 2, as Stop Inhibit signal was significantly higher in this scan, $p = .048$, but not in Scan 1, $p = .394$, corrected for multiple comparisons.

To evaluate the possibility that the higher BOLD signal in the Stop Inhibit compared with the Stop Respond trials was due to higher pretrial BOLD signal, we calculated the mean BOLD signal during the TR preceding trial onset for each trial type. This analysis revealed that the pretrial signal was in fact nonsignificantly lower in the Stop Inhibit compared with the Stop Respond trials, −0.036 (±0.269) and 0.013 (±0.212), respectively, $p = .546$, two-tailed. Therefore, it is unlikely that the level of pretrial BOLD signal is responsible for the greater activation of the STN in the Stop Inhibit trials.

### Early Activation of STN Inversely Correlates with SSRT

To determine the behavioral relevance of early left STN signaling in Stop Inhibit trials, we tested whether there was an association between individual differences in the differential STN signal in the Stop Inhibit compared with Stop Response trials (delta STN) in Scan 2 and the stop signal reaction time (SSRT). We focused on Scan 2 signal because this was the time point most responsible for the early activation of the STN in Stop Inhibit trials. The SSRT is a psychophysically derived estimate of the participant's RT to the auditory stop signal, with shorter SSRTs indicating faster ability to stop, as a shorter time interval is required to successfully integrate the stop signal in decision-making. We found a significant inverse relationship between delta STN and SSRT: $r = -.646$, $p = .004$. This relationship was not driven by outlier data, as evidenced by the correlation remaining significant when recomputed after iterative removal of single data points: $r > -.559$, $p < .020$.

## DISCUSSION

We investigated the role of the STN in behavioral inhibition in humans using a novel fMRI method for STN signal localization. We observed selective engagement of the STN, particularly in the right hemisphere, during Stop trials of the SST. The magnitude of STN signal correlated inversely with level of trait impulsivity measured by a well-validated personality questionnaire. The study also found evidence of early differential engagement of the STN during successful compared with unsuccessful Stop trials. Individual differences in the level of differential STN engagement were inversely correlated with the ability to stop quickly. Taken together, these results provide new insights into the mechanisms of STN-mediated stopping of action and link this structure's function with impulsivity.

One of the goals of this study was to validate a method for STN signal localization. The selective engagement of the STN during Stop trials has been observed by prior human fMRI studies employing the SST (Li et al., 2008; Aron & Poldrack, 2006). The consistency of the STN results between the present study with these studies

helps to validate our novel method for STN signal localization. Furthermore, these results add to the other lines of evidence from clinical (Obeso et al., 2014; Bickel et al., 2010; Frank et al., 2007) and animal (Eagle et al., 2008) research, supporting the proposition that the STN mediates behavioral inhibition.

The results of this study provide novel insights into STN involvement in behavioral inhibition. To the best of our knowledge, the time course results represent the first demonstration of enhanced STN activity during successful compared with unsuccessful Stop trials in humans. This demonstration provides stronger evidence that the STN mediates behavioral inhibition because it stands to reason that the inhibition signal would be greater during successful (Stop Inhibit) compared with unsuccessful (Stop Respond) trials. The inverse correlation between the magnitude of STN signal with SSRT, for example, participants with higher STN signal exhibited faster stopping, replicates a similar finding from a recent study (Jahfari et al., 2018) and provides behavioral validation of the proposition that STN mediates inhibition. It is notable that greater STN signal during successful Stop trials was detected in the time course and not the regression-based results. The latter is relatively insensitivity to subtle differences in the temporal pattern of BOLD signal. Thus, it is not surprising that the early rise in STN signal was observed only in the time series analysis.

The time course results provide mechanistic insights into how the STN may be promoting stopping. The fact that this heightened activity occurred early in the time course is consistent with the race model of inhibition (Logan et al., 1984). This model proposes that the execution or inhibition of an action is determined by a race between signals representing these alternatives. Signals for this race are thought to be coded within the so-called go and no go pathways of the BG (Schmidt, Leventhal, Mallet, Chen, & Berke, 2013; Kravitz et al., 2010; Frank, 2006), the latter of which the STN is a core member. The early STN activity in Stop Inhibit trials could signify the relay of the no go signal before the go signal to downstream effectors systems. This possibility is consistent with the results of a rodent study (Schmidt et al., 2013). As others have speculated (Aron & Poldrack, 2006) based on the relatively short timescale involved with the SST and studies suggesting insensitivity of the SSRT to striatal damage (Aron et al., 2003; Eagle & Robbins, 2003), the early activation of the STN is consistent with a hyperdirect pathway-mediated stopping mechanism. This pathway provides a short-latency, excitatory signal primarily from prefrontal structures to the STN (Nambu, Tokuno, & Takada, 2002), which could presumably drive the early STN signaling reported in this study.

A hyperdirect pathway mechanism of early activation of the STN is relevant to a discussion of the laterality of our findings. The early activation of the STN occurring on the left hemisphere may appear to be at odds with prior studies (Aron, Robbins, & Poldrack, 2014; Wessel, Conner, Aron, & Tandon, 2013; Swann et al., 2012; Aron & Poldrack, 2006) and our own regression-based results suggest that the right STN may be more critical for or robustly involved in inhibition. One explanation for these apparently divergent findings could be related to the fact that all task responses were given with the right hand in this study. This means that left-sided structures, including those in the BG, given the well-recognized contralateral control of motor functions (Benazzouz et al., 1996), would be better situated to transmit a rapid inhibition signal. However, this explanation does not account for studies that have required right-handed responses but did not find lateralized STN response patterns (Jahfari et al., 2018; Li et al., 2008; Aron & Poldrack, 2006). Future studies manipulating laterality of motor responses could test the hypothesis of contralateral STN early activation during successful stopping.

Prior fMRI studies using time course analysis have failed to find enhanced STN signal during successful compared with unsuccessful stop trials of the SST (Jahfari et al., 2018; de Hollander, Keuken, van der Zwaag, Forstmann, & Trampel, 2017; Aron & Poldrack, 2006). In fact, some studies found greater STN signal during unsuccessful compared with successful Stop trials (Jahfari et al., 2018; de Hollander et al., 2017), challenging the proposition that the STN is mediating inhibition. This pattern of results could be reconciled with this proposition by considering that additional cognitive processes are likely engaged by the STN in failed Stop trials. There is substantial evidence that the STN supports control processes, for example, "slow your horses" (Frank et al., 2007; Frank, 2006). Reactive control function of the STN could be triggered in unsuccessful Stop trials by the commission of an error, as when a motor response is executed despite the auditory stop signal occurring. Thus, the heightened STN BOLD signal in unsuccessful Stop trials could reflect STN engagement by both behavioral inhibition and reactive control processes.

A potential explanation for the divergence between the results of the present and prior studies is the method employed for STN signal localization. As others have noted (de Hollander et al., 2015), it is very challenging to image the STN because of its small size and close proximity to functionally heterogeneous structures such as the SN. Elements of our method may have limited the contamination of the STN signal with signal from nearby structures. In turn, this may have increased sensitivity to detect differential STN activity across the two types of Stop trials. These elements include utilizing unsmoothed images from which we derived STN activation estimates and drawing ROI masks directly from EPI volumes in "native space." The latter avoided signal localization errors that may stem from spatially transforming task EPI volumes onto template brains or coregistering task volumes to structural images.

The tSNR values we observed support the possibility that this study's signal localization method possesses enhanced power to detect STN. These values fall within a range that should allow for the detection of task-evoked BOLD signal changes in a reasonable amount of time (Murphy, Bodurka, & Bandettini, 2007) and are considerably higher than the tSNR values observed for other STN localization methods in 3T (de Hollander et al., 2017). Despite these appealing features, future studies will be required to directly compare our approach for STN signal localization with other methods to determine exactly how much it improves STN signal measurement accuracy.

The association between STN function and trait impulsivity adds this structure to the list of brain regions previously linked with impulsivity in humans, such as regions of the pFC (Horn, Dolan, Elliott, Deakin, & Woodruff, 2003), the striatum (Plichta & Scheres, 2014), and other subcortical regions (Brown, Manuck, Flory, & Hariri, 2006). This association also extends findings from the Parkinson STN deep brain stimulation literature (Frank et al., 2007), which demonstrated that the modulation of the STN in this condition promotes impulsive responding. This study's demonstration of a link between STN and trait impulsivity in a sample of healthy participants suggests that this link is not the result of, or limited to, situations involving STN pathology. The link with trait impulsivity, as measured by the TCI, suggests the STN shapes a variety of real-world behaviors, because the TCI derives its measure of impulsivity by surveying behavioral tendencies from a large and diverse set of real-world situations. However, the TCI is a self-report instrument, and thus, future studies utilizing objective measures will be required to test the possibility that the STN influences real-world impulsive behaviors and tendencies. Nonetheless, given the strong links between impulsivity and a number of psychiatric conditions (Strakowski et al., 2010; Swann et al., 2009; Nock & Kessler, 2006; Horesh et al., 1999; Barkley, 1997), including substance abuse (Ersche et al., 2010; de Wit, 2009), our results also suggest that STN dysfunction could be involved in the pathophysiology of these conditions. A goal of future studies could be to test STN function in clinical populations.

Another limitation of this study is the inability to investigate network influences on the STN. The STN is part of a distributed network of brain regions involved in behavioral inhibition (Aron, 2011). It is possible that the STN findings of this study were influenced by upstream regions from this network, such as regions of the pFC that have been shown to exhibit differential activity in successful versus unsuccessful Stop events (Wessel et al., 2013; Swann et al., 2012). However, elements of experimental design and scanning factors necessitated by our small voxel imaging method prevented us from directly testing for network influences on STN function. The study's rapid event-related trial design and the relatively sparse number of relevant prior trial–current trial type sequences prohibited the application of functional connectivity analyses capable of addressing these possibilities. Another factor was the restricted brain volume that was sampled. The relatively small voxel dimension necessitated by our STN localization method confers a tradeoff with the brain volume that could be acquired with TRs compatible with event-related fMRI studies.

In summary, this study utilized a novel method for STN signal localization in humans using fMRI to uncover novel mechanistic insights into STN function and links with impulsivity. The results of this study suggest that the STN is a critical element in behavioral inhibition, shaping a wide variety of behavioral tendencies with relevance to important neuropsychiatric conditions and states.

Reprint requests should be sent to Jong H. Yoon, 3801 Miranda Ave, Palo Alto, CA 94304, or via e-mail: jhyoon1@stanford.edu.

## REFERENCES

Aron, A. R. (2011). From reactive to proactive and selective control: Developing a richer model for stopping inappropriate responses. *Biological Psychiatry*, *69*, e55–e68.

Aron, A. R., & Poldrack, R. A. (2006). Cortical and subcortical contributions to stop signal response inhibition: Role of the subthalamic nucleus. *Journal of Neuroscience*, *26*, 2424–2433.

Aron, A. R., Robbins, T. W., & Poldrack, R. A. (2014). Inhibition and the right inferior frontal cortex: One decade on. *Trends in Cognitive Sciences*, *18*, 177–185.

Aron, A. R., Schlaghecken, F., Fletcher, P. C., Bullmore, E. T., Eimer, M., Barker, R., et al. (2003). Inhibition of subliminally primed responses is mediated by the caudate and thalamus: Evidence from functional MRI and Huntington's disease. *Brain*, *126*, 713–723.

Barkley, R. A. (1997). Behavioral inhibition, sustained attention, and executive functions: Constructing a unifying theory of ADHD. *Psychological Bulletin*, *121*, 65–94.

Benazzouz, A., Boraud, T., Feger, J., Burbaud, P., Bioulac, B., & Gross, C. (1996). Alleviation of experimental hemiparkinsonism by high-frequency stimulation of the subthalamic nucleus in primates: A comparison with L-Dopa treatment. *Movement Disorders*, *11*, 627–632.

Bickel, S., Alvarez, L., Macias, R., Pavon, N., Leon, M., Fernandez, C., et al. (2010). Cognitive and neuropsychiatric effects of subthalamotomy for Parkinson's disease. *Parkinsonism & Related Disorders*, *16*, 535–539.

Bronstein, J. M., Tagliati, M., Alterman, R. L., Lozano, A. M., Volkmann, J., Stefani, A., et al. (2011). Deep brain stimulation for Parkinson disease: An expert consensus and review of key issues. *Archives of Neurology*, *68*, 165.

Brown, S. M., Manuck, S. B., Flory, J. D., & Hariri, A. R. (2006). Neural basis of individual differences in impulsivity: Contributions of corticolimbic circuits for behavioral arousal and control. *Emotion*, *6*, 239–245.

Cloninger, C. R. (1994). *The Temperament and Character Inventory (TCI): A guide to its development and use* (1st ed.). St. Louis, MO: Center for Psychobiology of Personality, Washington University.

Coenen, V. A., Prescher, A., Schmidt, T., Picozzi, P., & Gielen, F. L. (2008). What is dorso-lateral in the subthalamic nucleus

(STN)?—A topographic and anatomical consideration on the ambiguous description of today's primary target for deep brain stimulation (DBS) surgery. *Acta Neurochirurgica (Wien)*, *150*, 1163–1165; discussion 1165.
de Hollander, G., Keuken, M. C., & Forstmann, B. U. (2015). The subcortical cocktail problem; mixed signals from the subthalamic nucleus and substantia nigra. *PLoS One*, *10*, e0120572.
de Hollander, G., Keuken, M. C., van der Zwaag, W., Forstmann, B. U., & Trampel, R. (2017). Comparing functional MRI protocols for small, iron-rich basal ganglia nuclei such as the subthalamic nucleus at 7 T and 3 T. *Human Brain Mapping*, *38*, 3226–3248.
de Wit, H. (2009). Impulsivity as a determinant and consequence of drug use: A review of underlying processes. *Addiction Biology*, *14*, 22–31.
Dexter, D. T., Carayon, A., Javoy-Agid, F., Agid, Y., Wells, F. R., Daniel, S. E., et al. (1991). Alterations in the levels of iron, ferritin and other trace metals in Parkinson's disease and other neurodegenerative diseases affecting the basal ganglia. *Brain*, *114*, 1953–1975.
Dormont, D., Ricciardi, K. G., Tandé, D., Parain, K., Menuel, C., Galanaud, D., et al. (2004). Is the subthalamic nucleus hypointense on T2-weighted images? A correlation study using MR imaging and stereotactic atlas data. *American Journal of Neuroradiology*, *25*, 1516–1523.
Eagle, D. M., Baunez, C., Hutcheson, D. M., Lehmann, O., Shah, A. P., & Robbins, T. W. (2008). Stop-signal reaction-time task performance: Role of prefrontal cortex and subthalamic nucleus. *Cerebral Cortex*, *18*, 178–188.
Eagle, D. M., & Robbins, T. W. (2003). Lesions of the medial prefrontal cortex or nucleus accumbens core do not impair inhibitory control in rats performing a stop-signal reaction time task. *Behavioral Brain Research*, *146*, 131–144.
Eklund, A., Nichols, T. E., & Knutsson, H. (2016). Cluster failure: Why fMRI inferences for spatial extent have inflated false-positive rates. *Proceedings of the National Academy of Sciences, U.S.A.*, *113*, 7900–7905.
Ersche, K. D., Turton, A. J., Pradhan, S., Bullmore, E. T., & Robbins, T. W. (2010). Drug addiction endophenotypes: Impulsive versus sensation-seeking personality traits. *Biology Psychiatry*, *68*, 770–773.
Forstmann, B. U., Keuken, M. C., Jahfari, S., Bazin, P. L., Neumann, J., Schafer, A., et al. (2012). Cortico-subthalamic white matter tract strength predicts interindividual efficacy in stopping a motor response. *Neuroimage*, *60*, 370–375.
Frank, M. J. (2006). Hold your horses: A dynamic computational role for the subthalamic nucleus in decision making. *Neural Network*, *19*, 1120–1136.
Frank, M. J., Samanta, J., Moustafa, A. A., & Sherman, S. J. (2007). Hold your horses: Impulsivity, deep brain stimulation, and medication in parkinsonism. *Science*, *318*, 1309–1312.
Glover, G. H. (1999). Deconvolution of impulse response in event-related BOLD fMRI. *Neuroimage*, *9*, 416–429.
Haacke, E. M., Cheng, N. Y., House, M. J., Liu, Q., Neelavalli, J., Ogg, R. J., et al. (2005). Imaging iron stores in the brain using magnetic resonance imaging. *Magnetic Resonance Imaging*, *23*, 1–25.
Horesh, N., Gothelf, D., Ofek, H., Weizman, T., & Apter, A. (1999). Impulsivity as a correlate of suicidal behavior in adolescent psychiatric inpatients. *Crisis*, *20*, 8–14.
Horn, N. R., Dolan, M., Elliott, R., Deakin, J. F., & Woodruff, P. W. (2003). Response inhibition and impulsivity: An fMRI study. *Neuropsychologia*, *41*, 1959–1966.
Jahfari, S., Ridderinkhof, K. R., Collins, A. G. E., Knapen, T., Waldorp, L. J., & Frank, M. J. (2018). Cross-task contributions of frontobasal ganglia circuitry in response inhibition and conflict-induced slowing. *Cerebral Cortex*, *4*, 95.
Kravitz, A. V., Freeze, B. S., Parker, P. R., Kay, K., Thwin, M. T., Deisseroth, K., et al. (2010). Regulation of parkinsonian motor behaviours by optogenetic control of basal ganglia circuitry. *Nature*, *466*, 622–626.
Li, C. S., Yan, P., Sinha, R., & Lee, T. W. (2008). Subcortical processes of motor response inhibition during a stop signal task. *Neuroimage*, *41*, 1352–1363.
Logan, G. D., Cowan, W. B., & Davis, K. A. (1984). On the ability to inhibit simple and choice reaction time responses: A model and a method. *Journal of Experimental Psychology, Human Perception and Performance*, *10*, 276–291.
Murphy, K., Bodurka, J., & Bandettini, P. A. (2007). How long to scan? The relationship between fMRI temporal signal to noise ratio and necessary scan duration. *Neuroimage*, *34*, 565–574.
Nambu, A., Tokuno, H., & Takada, M. (2002). Functional significance of the cortico-subthalamo-pallidal 'hyperdirect' pathway. *Neuroscience Research*, *43*, 111–117.
Niemann, K., & van Nieuwenhofen, I. (1999). One atlas—three anatomies: Relationships of the Schaltenbrand and Wahren microscopic data. *Acta Neurochirurgica (Wien)*, *141*, 1025–1038.
Nock, M. K., & Kessler, R. C. (2006). Prevalence of and risk factors for suicide attempts versus suicide gestures: Analysis of the National comorbidity survey. *Journal of Abnormal Psychology*, *115*, 616–623.
Nowinski, W. L. (1998). Anatomical targeting in functional neurosurgery by the simultaneous use of multiple Schaltenbrand-Wahren brain atlas microseries. *Stereotactic and Functional Neurosurgery*, *71*, 103–116.
Obeso, I., Wilkinson, L., Casabona, E., Speekenbrink, M., Luisa Bringas, M., Alvarez, M., et al. (2014). The subthalamic nucleus and inhibitory control: Impact of subthalamotomy in Parkinson's disease. *Brain*, *137*, 1470–1480.
Plichta, M. M., & Scheres, A. (2014). Ventral-striatal responsiveness during reward anticipation in ADHD and its relation to trait impulsivity in the healthy population: A meta-analytic review of the fMRI literature. *Neuroscience Biobehavioral Reviews*, *38*, 125–134.
Richter, E. O., Hoque, T., Halliday, W., Lozano, A. M., & Saint-Cyr, J. A. (2004). Determining the position and size of the subthalamic nucleus based on magnetic resonance imaging results in patients with advanced Parkinson disease. *Journal of Neurosurgery*, *100*, 541–546.
Schafer, A., Forstmann, B. U., Neumann, J., Wharton, S., Mietke, A., Bowtell, R., et al. (2011). Direct visualization of the subthalamic nucleus and its iron distribution using high-resolution susceptibility mapping. *Human Brain Mapping*, *33*, 2831–2842.
Schaltenbrand, G., Hassler, R. G., & Wahren, W. (1977). *Atlas for stereotaxy of the human brain* (2nd rev. and enl. ed.). Stuttgart: Thieme.
Schmidt, R., Leventhal, D. K., Mallet, N., Chen, F., & Berke, J. D. (2013). Canceling actions involves a race between basal ganglia pathways. *Nature Neuroscience*, *16*, 1118–1124.
Sofic, E., Paulus, W., Jellinger, K., Riederer, P., & Youdim, M. B. (1991). Selective increase of iron in substantia nigra zona compacta of parkinsonian brains. *Journal of Neurochemistry*, *56*, 978–982.
Strakowski, S. M., Fleck, D. E., DelBello, M. P., Adler, C. M., Shear, P. K., Kotwal, R., et al. (2010). Impulsivity across the course of bipolar disorder. *Bipolar Disorders*, *12*, 285–297.
Swann, N. C., Cai, W., Conner, C. R., Pieters, T. A., Claffey, M. P., George, J. S., et al. (2012). Roles for the pre-supplementary motor area and the right inferior frontal gyrus in stopping

action: Electrophysiological responses and functional and structural connectivity. *Neuroimage*, *59*, 2860–2870.
Swann, A. C., Lijffijt, M., Lane, S. D., Steinberg, J. L., & Moeller, F. G. (2009). Increased trait-like impulsivity and course of illness in bipolar disorder. *Bipolar Disorders*, *11*, 280–288.
Wessel, J. R., Conner, C. R., Aron, A. R., & Tandon, N. (2013). Chronometric electrical stimulation of right inferior frontal cortex increases motor braking. *Journal Neuroscience*, *33*, 19611–19619.
Yoon, J. H., Larson, P., Grandelis, A., La, C., Cui, E., Carter, C. S., et al. (2015). Delay period activity of the substantia nigra during proactive control of response selection as determined by a novel fMRI localization method. *Journal of Cognitive Neuroscience*, *27*, 1238–1248.
Yushkevich, P. A., Piven, J., Hazlett, H. C., Smith, R. G., Ho, S., Gee, J. C., et al. (2006). User-guided 3D active contour segmentation of anatomical structures: Significantly improved efficiency and reliability. *Neuroimage*, *31*, 1116–1128.